Underdamped stochastic thermodynamic engines in contact with a heat bath with arbitrary temperature profile

Olga Movilla Miangolarra, ¹ Rui Fu, ¹ Amirhossein Taghvaei ⁰, ¹ Yongxin Chen, ² and Tryphon T. Georgiou ⁰ ¹ Department of Mechanical and Aerospace Engineering, University of California, Irvine, California 92697, USA ² School of Aerospace Engineering, Georgia Institute of Technology, Atlanta, Georgia 30332, USA

(Received 13 January 2021; accepted 14 May 2021; published 1 June 2021)

We study thermodynamic processes in contact with a heat bath that may have an arbitrary time-varying periodic temperature profile. Within the framework of stochastic thermodynamics, and for models of thermodynamic engines in the idealized case of underdamped particles in the low-friction regime subject to a harmonic potential, we derive explicit bounds as well as optimal control protocols that draw maximum power and achieve maximum efficiency at any specified level of power.

DOI: 10.1103/PhysRevE.103.062103

I. INTRODUCTION

For more than 200 years, Carnot's idealized concept of a heat engine [1] has been the cornerstone of equilibrium thermodynamics [2]. It provided a standard as well as led to the discovery of the absolute temperature scale, entropy, and the second law of thermodynamics. The sequel, beyond equilibrium and quasistatic operation, proved a challenging one. Statistical mechanics and stochastic fluctuation theories have since, and for over a hundred years, been advancing our insight into the irreversibility of nonequilibrium thermodynamic transitions. In this endeavor, a particular promising model of far-from-equilibrium transitions is that of stochastic thermodynamics (also stochastic energetics) [3–6] that followed at the heels of fluctuation theories [7–11].

In the present work we adopt the framework of stochastic thermodynamics so as to quantify the amount of power as well as the efficiency that thermodynamic engines can achieve when harvesting energy from a heat bath with an arbitrary but periodically fluctuating temperature profile. Our study is expected to be of value, in particular, to theorists and engineers that work with nano machines and nano sensing devices at the scale of molecular and thermal fluctuations. Specifically, in our work, the Langevin equation

$$dX_t = v_t dt (1a)$$

$$mdv_t = -\nabla_x U(t, X_t)dt - \gamma v_t dt + \sqrt{2\gamma k_B T(t)}dB_t, \quad (1b)$$

provides a model for a molecular system that interacts with a thermal environment. In this, $X_t \in \mathbb{R}$ denotes the location of a particle (which is taken to be one-dimensional for notational simplicity), $v_t \in \mathbb{R}$ represents its velocity at time t, m its mass, γ the viscosity coefficient of an ambient medium, k_B the Boltzmann constant, T(t) the time-varying temperature of the heat bath at time t that a statistical ensemble of particles is in contact with, B_t a standard Brownian motion that represents thermal excitation from a heat bath, and U(t, x)

a time-varying potential exerting a force $-\nabla_x U(t,x)$ on a particle at location $x \in \mathbb{R}$. This potential represents a control action that models interaction of our ensemble of particles with the external world.

This Langevin model has been extensively used to describe heat engines in a Carnot-like cycle, that cycles through contact with heat baths of different temperature, in order to quantify maximum power that can be drawn as well as efficiency at maximum power. Specifically, foundational work has been carried out in the overdamped regime [12–14] where inertial effects are neglected, as well as in the underdamped regime [15,16] under a low-friction assumption, where inertial effects now dominate dissipation. Most importantly, experimental realization and verification of findings have been reported in different settings [17–19].

Energy and entropy exchange between a heat bath and a particle ensemble is not particular to (thermodynamic) engines. Fluctuations in chemical concentrations in conjunction with the variability of electrochemical potentials may provide a universal source of cellular energy [20]. Indeed, a similar mechanism appears to be at play in biological engines. In these, energy exchange appears to be mediated by continuous processes and energy differentials [21], in contrast to the classical Carnot cycle which alternates between heat baths of constant temperature in an idealized engine. Thus, as contemplated by E. Schrödinger [22,23], the ability of life to maintain a distance from equilibrium may be tied to mechanisms that allow drawing energy out of naturally or self-induced fluctuating temperature or chemical concentrations.

It is partly the above circle of ideas that led us to consider the rudimentary model of a cyclic process (periodical temperature profile of a heat bath) that fuels a molecular engine represented by stochastically driven Langevin dynamics. Another paradigm that may provide context is that of molecular engines that may some day be engineered to tap onto cyclic temperature fluctuations for work production. The work we present below is an extension of recent studies for periodic temperature profile in the linear regime [24–26]. It addresses the nonlinear regime and, in particular, the case of underdamped dynamics where the low-friction assumption applies.

II. ENERGETICS AND LOW-FRICTION APPROXIMATION

Throughout the paper we will consider the Langevin dynamics (1) with a harmonic potential

$$U(t,x) = \frac{1}{2}q(t)x^2,$$

where q(t) represents its intensity and constitutes our control variable. The total energy of a particle is the sum of kinetic and potential energies,

$$E_t = \frac{1}{2} m v_t^2 + \frac{1}{2} q(t) X_t^2.$$

The work and heat exchange at the level of a single particle, dW_t and dQ_t , respectively, are [3]

$$dW_t = \frac{1}{2}\dot{q}(t)X_t^2 dt, \tag{2a}$$

$$dQ_t = -\gamma v_t^2 dt + \frac{\gamma k_B T(t)}{m} dt + \sqrt{2\gamma k_B T(t)} v_t dB_t.$$
 (2b)

These definitions are in agreement with the first law of thermodynamics, i.e., dE = dQ + dW. Taking the expectation of (2) yields the average rate of work and heat exchange,

$$d\mathcal{W}_t = \frac{1}{2}\dot{q}(t)\Sigma_x(t)dt, \qquad (3a)$$

$$d\mathcal{Q}_t = \left[-\gamma \Sigma_v(t) + \frac{\gamma k_B T(t)}{m} \right] dt, \tag{3b}$$

where Σ_x and Σ_v are the variances of X_t and v_t , respectively. The averaged expressions also satisfy the first law of thermodynamics $d\mathcal{E}_t = d\mathcal{Q}_t + d\mathcal{W}_t$, where

$$\mathcal{E}_t = \frac{1}{2}q(t)\Sigma_x(t) + \frac{1}{2}m\Sigma_v(t)$$

is the average total energy of the particle.

The governing equations for the variance are obtained from the Langevin dynamics (1),

$$\dot{\Sigma}_x(t) = 2\Sigma_{xv}(t),\tag{4a}$$

$$\dot{\Sigma}_{xv}(t) = \Sigma_v(t) - \frac{q(t)}{m} \Sigma_x(t) - \frac{\gamma}{m} \Sigma_{xv}(t), \tag{4b}$$

$$\dot{\Sigma}_{v}(t) = -\frac{2q(t)}{m} \Sigma_{xv}(t) - \frac{2\gamma}{m} \Sigma_{v}(t) + \frac{2\gamma k_{B}}{m^{2}} T(t), \quad (4c)$$

where $\Sigma_{xv}(t)$ is the correlation between X_t and v_t .

Although the differential equations for the evolution of the variance are explicit and in closed-form, the analysis for maximizing efficiency is still challenging due to the presence of the three coupled ODEs. As a result, it is common to consider simplifying approximations that hold in different physical regimes.

Our analysis concerns the underdamped (or low-friction) regime that is studied in Refs. [15,16]. When the temperature T(t) and the harmonic potential intensity q(t) are constant, the low-friction regime holds when the particle in (1) undergoes many oscillations before dissipation effects become significant. Mathematically, this amounts to $\sqrt{\frac{q}{m}} \gg \frac{\gamma}{m}$. In the case where T(t) and q(t) are time varying periodic functions, it

is required in addition that their power spectrum mostly lies below the natural frequency of oscillations $\sqrt{q/m}$.

Under the low-friction assumptions, the equipartition condition

$$\frac{1}{2}q(t)\Sigma_x(t) = \frac{1}{2}m\Sigma_v(t) \tag{5}$$

holds approximately [16, Section 4.2]. As a result, it is possible to express the dynamics of our system as a function of $\Sigma_{v}(t)$ uniquely. More precisely, we can use (4a) to express $\Sigma_{xv}(t)$ as follows:

$$\Sigma_{xv}(t) = \frac{1}{2}\dot{\Sigma}_x = \frac{m}{2q(t)}\dot{\Sigma}_v - \frac{m\dot{q}(t)}{2q(t)^2}\Sigma_v,$$

where the second equality comes from the equipartition condition (5). Now, we can rewrite $\Sigma_{xy}(t)$ in (4c), to obtain

$$\dot{\Sigma}_v(t) = \Sigma_v(t) \left[\frac{\dot{q}(t)}{2q(t)} - \frac{\gamma}{m} \right] + \frac{\gamma k_B}{m^2} T(t).$$
 (6)

For this equation to be meaningful, we require q(t) to be (weakly) differentiable. Equation (6) is the underlying model for our analysis through the rest of the paper.

III. ANALYSIS OF MAXIMUM POWER

We consider a stochastic thermodynamic engine driven by a periodic temperature T(t) with period t_f . The averaged power output over a cycle is equal to

$$\mathcal{P} = -\frac{1}{t_f} \int_0^{t_f} d\mathcal{W}_t.$$

Using the first law of thermodynamics $d\mathcal{E}_t = d\mathcal{Q}_t + d\mathcal{W}_t$, the power can be expressed in terms of heat exchange as follows:

$$\mathcal{P} = \frac{1}{t_f} \int_0^{t_f} (d \mathcal{Q}_t - d \mathcal{E}_t)$$

$$= \frac{\gamma}{t_f} \int_0^{t_f} \left[\frac{k_B T(t)}{m} - \Sigma_v(t) \right] dt + \frac{1}{t_f} [\mathcal{E}(t_f) - \mathcal{E}(0)], \quad (7)$$

where the definition (3b) is used and $\mathcal{E}_t \equiv \mathcal{E}(t)$, for clarity. To account for possible discontinuities in T(t) and q(t), as it is often the case in the underdamped setting [15,27,28], we consider a cycle from 0^+ to t_f^+ . Thus, q, Σ_v , and \mathcal{E} , which are periodic, satisfy

$$q(0^+) = q(t_f^+)$$
 and $\Sigma_v(0^+) = \Sigma_v(t_f^+),$ (8)

and $\mathcal{E}(0^+) = \mathcal{E}(t_f^+)$. The latter condition removes the boundary terms in (7), while conditions (8) impose an integral constraint on $\Sigma_v(t)$. Specifically, if we divide (6) by $\Sigma_v(t)$ and integrate from 0^+ to t_f^+ we obtain

$$\log \left[\frac{\Sigma_{v}(t_{f}^{+})}{\Sigma_{v}(0^{+})} \right] = \log \left[\frac{q(t_{f}^{+})}{q(0^{+})} \right]^{\frac{1}{2}} - \frac{\gamma}{m} t_{f} + \frac{\gamma k_{B}}{m^{2}} \int_{0}^{t_{f}} \frac{T(t)}{\Sigma_{v}(t)} dt.$$
(9)

Thus, in view of (8).

$$\int_0^{t_f} \frac{T(t)}{\Sigma_v(t)} dt = \frac{mt_f}{k_B}.$$
 (10)

This integral constraint is the main ingredient in our analysis for both maximum power and maximum efficiency.

We first consider maximizing power output, namely,

$$\max_{\Sigma_v(\cdot)} \frac{\gamma}{t_f} \int_0^{t_f} \left[\frac{k_B T(t)}{m} - \Sigma_v(t) \right] dt, \tag{11}$$

subject to the constraint (10). We observe that due to (10),

$$\int_0^{t_f} \Sigma_v(t) dt = \int_0^{t_f} \left[\Sigma_v(t) + c \frac{T(t)}{\Sigma_v(t)} \right] dt - c \frac{mt_f}{k_B}$$

for any arbitrary constant c. The minimal value for the integrand $\Sigma_v(t) + c \frac{T(t)}{\Sigma_v(t)}$, pointwise and with respect to $\Sigma_v(t)$, is attained for $\Sigma_v(t) = \sqrt{cT(t)}$. This choice for $\Sigma_v(t)$ also satisfies (10) for $\sqrt{c} = \frac{k_B}{mt_f} \int_0^{t_f} \sqrt{T(t)} dt$. Therefore,

$$\Sigma_v(t) = \left[\frac{k_B}{mt_f} \int_0^{t_f} \sqrt{T(s)} ds\right] \sqrt{T(t)}$$
 (12)

is the unique maximizer of (11).

The relation between $\Sigma_v(t)$ and the protocol q(t) can be obtained from (6) by direct integration (cf. (9)), which for the optimizing $\Sigma_v(\cdot)$ gives

$$q(t) = q_0 \frac{T(t)}{T(0)} \exp\left\{ \frac{2\gamma t_f}{m} \left[\frac{t}{t_f} - \frac{\int_0^t \sqrt{T(s)} ds}{\int_0^{t_f} \sqrt{T(s)} ds} \right] \right\}. \quad (13)$$

Note that, q_0 specifies the starting value q(0) of the optimal protocol. Further, q(t) is continuous at all times when T(t) is, which agrees with the intuition that jumps in the control are necessitated for adapting to a sudden jump in temperature [12,15].

Finally, inserting (12) into the expression for power, we obtain that, under this protocol, any value for q_0 gives the same level of power, namely,

$$\mathcal{P}^* = \frac{\gamma k_B}{m} \text{Var}(\sqrt{T})$$
 (14)

where

$$\operatorname{Var}(\sqrt{T}) = \frac{1}{t_f} \int_0^{t_f} T(t)dt - \left[\frac{1}{t_f} \int_0^{t_f} \sqrt{T(t)}dt \right]^2$$

quantifies fluctuations in $\sqrt{T(t)}$.

Thus, expression (14) quantifies the maximum power that can be drawn in terms of an explicit measure of temperature fluctuations.

It is interesting to consider the shape of temperature fluctuations that allows maximum power to be drawn under the optimal protocol. In view of the above, it is easy to see that when $T(t) \in [T_c, T_h]$, the Carnot temperature profile

$$T_{\text{Carnot}}(t) = \begin{cases} T_h, & t \in \left[0, \frac{t_f}{2}\right) \\ T_c, & t \in \left[\frac{t_f}{2}, t_f\right), \end{cases}$$
(15)

allows drawingmaximum power, which in this case is

$$\frac{\gamma k_B}{m} \frac{(\sqrt{T_h} - \sqrt{T_c})^2}{4}.$$

This special profile (Carnot) has already been studied in Ref. [15].

IV. ANALYSIS OF MAXIMUM EFFICIENCY AT FIXED POWER

The classical definition of efficiency is the ratio of work produced over the amount of heat drawn from the hot bath into the system,

$$\eta_{\mathcal{Q}} = \frac{-\mathcal{W}}{\mathcal{Q}_h}.\tag{16}$$

This definition presumes that the environment that constitutes the hot heat bath is well defined, and as a consequence that Q_h is well defined as well. This is clearly the case for a Carnot cycle, $T(t) = T_{\text{Carnot}}(t)$, when the system remains in contact with the bath at T_h during the interval $[0, \frac{t_f}{2})$.

For this case, at maximum power,

$$\mathcal{Q}_h = \int_0^{\frac{r_f}{2}} d\mathcal{Q}_t = \frac{\gamma k_B}{m} \frac{t_f}{4} \sqrt{T_h} (\sqrt{T_h} - \sqrt{T_c}),$$

where the second equality is obtained using (3b) and the optimal expression for Σ_{ν} in (12). It follows that

$$\eta_{\mathcal{Q}} = 1 - \sqrt{\frac{T_c}{T_h}},$$

which is precisely the Curzon-Ahlborn efficiency [29,30]. This result was obtained in Ref. [15].

However, in the setting of an arbitrary periodic temperature profile, it is not entirely clear what constitutes the hot bath. The same bath serves as hot and cold, at different times, and therefore Q_h and η_Q may be given different definitions and be subject to different interpretations [24,26].

In the present work, following Ref. [26], we adopt

$$\eta_{\mathcal{U}} = \frac{-\mathcal{W}}{\mathcal{U}},$$

as our definition of efficiency, where

$$\mathcal{U} = -k_B \int_0^{t_f} S(\rho_t) \dot{T}(t) dt,$$

[also $\mathcal{U} = k_B \int T(t) \dot{S}(\rho_t) dt$, using integration by parts] represents the effective uptake of thermal energy, while

$$S(\rho_t) = -\iint \rho_t(x, v) \log[\rho_t(x, v)] dx dv$$

denotes the entropy of the particle-distribution ρ_t . The value \mathcal{U} can be thought of as the maximal amount of work that can be extracted when the dissipation is zero and the transition takes place quasistatically. In general, over a cycle,

$$\mathcal{U} = -\mathcal{W} + \mathcal{W}_{diss}$$

where the dissipation

$$W_{\text{diss}} = \int k_B T(t) \underbrace{\left[\dot{S}(\rho_t) dt - \frac{dQ}{k_B T(t)} \right]}_{\dot{S}},$$

relates to the total entropy production rate \dot{S}_{total} in the system and the environment. For quasistatic transitions $\mathcal{W}_{\text{diss}} = 0$ and n = 1.

In the underdamped low-friction regime with quadratic potential, the distribution ρ_t is Gaussian with independent

components (x, v) whose covariance are $\Sigma_x(t)$ and $\Sigma_v(t)$, respectively. Using the standard formula for the entropy of Gaussian distributions together with the equipartition condition (5) expressed in terms of the variances, \mathcal{U} simplifies to

$$\mathcal{U} = -\frac{k_B}{2} \int_0^{t_f} \ln \left[(2\pi e)^2 \frac{m}{q(t)} \Sigma_v^2(t) \right] \dot{T}(t) dt.$$

In case T(t) is discontinuous, the limits of integration need to be taken as 0^+ and t_f^+ , and similarly in what follows. Integration by parts gives

$$\mathcal{U} = \frac{k_B}{2} \int_0^{t_f} \left[2 \frac{\dot{\Sigma}_v(t)}{\Sigma_v(t)} - \frac{\dot{q}(t)}{q(t)} \right] T(t) dt$$
$$= \frac{k_B^2 \gamma}{m^2} \int_0^{t_f} \frac{T(t)^2}{\Sigma_v(t)} dt - \frac{k_B \gamma}{m} \int_0^{t_f} T(t) dt,$$

where we have used (6) to establish the second equality.

We now seek to optimize efficiency at a given power. To this end, it suffices to minimize the dissipation \mathcal{U} subject to the given power. Thus, we consider

$$\min_{\Sigma_v(\cdot)} \int_0^{t_f} \frac{T(t)^2}{\Sigma_v(t)} dt, \tag{17}$$

subject to (10) together with

$$\frac{\gamma}{t_f} \int_0^{t_f} \left[\frac{k_B T(t)}{m} - \Sigma_v(t) \right] dt = \mathcal{P},$$

for any given level of power \mathcal{P} . We follow a variational approach. The Lagrangian for our optimization problem is

$$\mathcal{L} = \frac{T(t)^2}{\Sigma_v(t)} + \lambda \left[\Sigma_v(t) - \frac{k_B T(t)}{m} + \frac{\mathcal{P}}{\gamma} \right] + \mu \left[\frac{T(t)}{\Sigma_v(t)} - \frac{m}{k_B} \right],$$

where λ , μ are the Lagrange multipliers. The stationarity condition for $\Sigma_v(t)$ gives

$$\Sigma_v(t) = \frac{1}{\sqrt{\lambda}} \sqrt{T(t)^2 + \mu T(t)}.$$

Applying the power constraint we obtain

$$\sqrt{\lambda} = \frac{\int_0^{t_f} \sqrt{T(t)^2 + \mu T(t)} dt}{\frac{k_B}{m} \int_0^{t_f} T(t) dt - \frac{t_f}{\nu} \mathcal{P}}.$$

In a similar manner as before, the optimal protocol can now be obtained by direct integration of (6), to give

$$q(t) = q_0 \frac{T(t)^2 + \mu T(t)}{T(0)^2 + \mu T(0)} \exp\left\{\frac{2\gamma [t - r(t)]}{m}\right\}, \quad (18)$$

where

$$r(t) = \frac{\int_0^{t_f} \sqrt{T(s)^2 + \mu T(s)} ds}{\int_0^{t_f} T(s) ds - \frac{t_f m}{\sqrt{k_o}} \mathcal{P}} \int_0^t \frac{\sqrt{T(s)}}{\sqrt{T(s) + \mu}} ds.$$

It now remains to fix μ by imposing the last constraint, which yields $r(t_f) = t_f$. This is,

$$\int_{0}^{t_{f}} \sqrt{T(t)^{2} + \mu T(t)} dt \int_{0}^{t_{f}} \frac{\sqrt{T(t)}}{\sqrt{T(t) + \mu}} dt$$

$$= t_{f} \int_{0}^{t_{f}} T(t) dt - \frac{t_{f}^{2} m}{\nu k_{B}} \mathcal{P}.$$
(19)

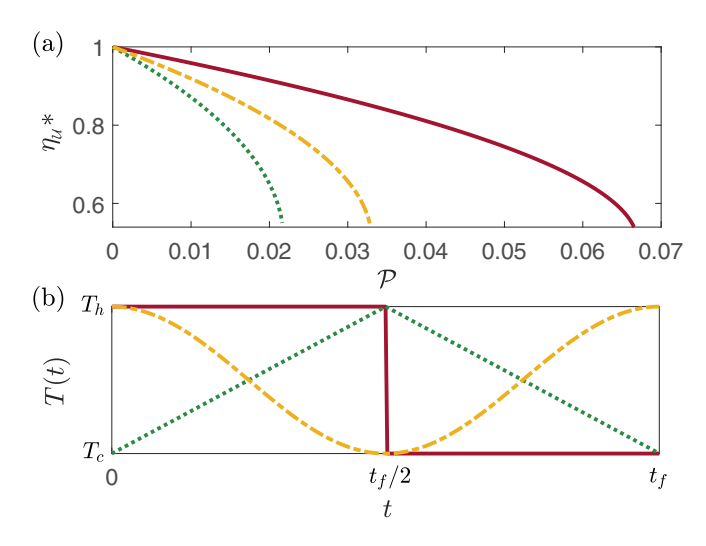


FIG. 1. (a) Maximum efficiency at fixed power for the temperature profiles portrayed in (b). (b) Temperature profiles with colors and patterns matching the corresponding performance curves in (a).

In general, Eq. (19) cannot be solved explicitly for μ . However, it is easily seen that when $\mathcal{P}=0$, then $\mu=0$ is a solution. Also, as $\mathcal{P}\to\mathcal{P}^*$, then the solution $\mu\to\infty$. It is worthwhile to point out that the condition $r(t_f)=t_f$ makes the protocol (18) continuous for continuous temperature profiles.

For notational convenience, we let

$$\overline{g(t)} = \frac{1}{t_f} \int_0^{t_f} g(t) dt$$

denote the average of a periodic function g(t) over the period. Now, putting all of the ingredients together, the optimal \mathcal{U} is

$$\mathcal{U}^* = \frac{t_f}{\kappa} \left(\frac{\sqrt{[T(t) + \mu]T(t)}}{\overline{T(t)} - \kappa \mathcal{P}} \times \overline{\left\{ \frac{T(t)^{\frac{3}{2}}}{\sqrt{[T(t) + \mu]}} \right\}} - \overline{T(t)} \right).$$

where $\kappa = m/(\gamma k_B)$. Consequently, the maximum efficiency at fixed power is

$$\eta_{\mathcal{U}}^{*}(\mathcal{P}) = \frac{\kappa \mathcal{P}}{\left(\frac{\sqrt{[T(t)+\mu]T(t)}}{T(t)-\kappa \mathcal{P}} \times \left\{\frac{T(t)^{\frac{3}{2}}}{\sqrt{[T(t)+\mu]}}\right\} - \overline{T(t)}\right)}.$$
 (20)

Figure 1 displays the trade-off between power and efficiency for three different temperature profiles. Note that for vanishing power we obtain the maximum possible efficiency, i.e., $\eta_u^* = 1$, that corresponds to vanishing dissipation. On the other hand, as $\kappa \mathcal{P} \to \kappa \mathcal{P}^* = \text{Var}(\sqrt{T})$ (from (14)), the limiting value from (20) gives that

$$\eta_{u}^{*} \to \frac{\sqrt{T(t)} \operatorname{Var}(\sqrt{T})}{T(t)^{\frac{3}{2}} - \overline{T(t)} \times \sqrt{T(t)}}.$$
(21)

This is precisely the efficiency at maximum power obtained by using the optimal protocol (13). The limit in (21) can also be expressed in terms of the third moment of the square root of the temperature

$$\mu_3(\sqrt{T}) = \frac{1}{t_f} \int_0^{t_f} [\sqrt{T(t)} - \overline{\sqrt{T(t)}}]^3 dt,$$

specifically,

$$\eta_{\mathcal{U}}^* \to \frac{1}{2 + \frac{\mu_3(\sqrt{T})}{\text{Var}(\sqrt{T})\sqrt{T(t)}}}.$$
 (22)

Thus, for any temperature profile such that $\mu_3(\sqrt{T}) = 0$, the limit is $\frac{1}{2}$, which in particular is true for the Carnot-like temperature profile $T(t) = T_{\text{Carnot}}(t)$. We also note that the third moment can be negative, leading to efficiency that exceeds $\frac{1}{2}$, albeit at the cost of decreasing maximum power.

V. EXAMPLE: SINUSOIDAL TEMPERATURE PROFILE

In the following we compare our results to the ones obtained in the linear response regime, where it is assumed that $T_h - T_c \ll T_h + T_c$ [24,31]. To this end, we consider the sinusoidal temperature profile

$$T(t) = \frac{T_h + T_c}{2} + \frac{T_h - T_c}{2} \cos(\omega t), \tag{23}$$

with $\omega \ll \sqrt{\frac{q}{m}}$ so as to ensure that the low-friction assumption holds.

We first use our analytical result to recover the expressions obtained in the linear response regime. Specifically, assuming $\Delta T = \frac{T_h - T_c}{2}$ is much smaller than $\bar{T} = \frac{T_h + T_c}{2}$, we have that

$$q^*(t) = q_0 + q_0 \frac{\Delta T}{\bar{T}} \cos(\omega t) + O(\Delta T^2),$$

$$\mathcal{P}^* = \frac{\gamma k_B}{8m} \frac{\Delta T^2}{\bar{T}} + O(\Delta T^3),$$

$$\eta_{\iota \iota}^*(\mathcal{P}^*) = \frac{1}{2} + O(\Delta T^2),$$

where the first two coincide with the expressions for the optimal protocol and power that are given in Refs. [24,31], in the limit where $\frac{q_0}{m}$ is large enough to satisfy the requirements of the low-friction regime. In fact, in the linear response regime $\eta_{\mathcal{U}}^*(\mathcal{P}^*) = \frac{1}{2} + O(\Delta T^2)$ holds for any temperature profile whose time-dependent component is an odd function of t.

Moreover, in order to illustrate the utility of our results, we compare the optimality of the protocol obtained in this paper, to the one obtained in the linear response regime. Specifically, we solve numerically the equations for the variance (4) for two protocols:

- (i) the optimal protocol obtained with low-friction assumption according to (13),
- (ii) the optimal protocol obtained in linear response regime in Ref. [24] and Ref. [31, Eqs. (29) and (30a)].

These two protocols, along with the temperature profile, are shown in Fig. 2. Then, we use the numerical solution to the equations for the variance to compute power and efficiency. The result, as the temperature difference $T_h - T_c$ is varied, is shown in Fig. 3.

In these numerical examples, we made sure $\frac{\gamma}{m} \ll \sqrt{\frac{q}{m}}$ so that the low-friction assumption remains valid. As it is expected, the optimal protocol under the linear response regime assumption performs well when the temperature ratio is small, giving a numerical result that agrees with Eqs. (13) and (20). However, as the temperature ratio increases, higher order

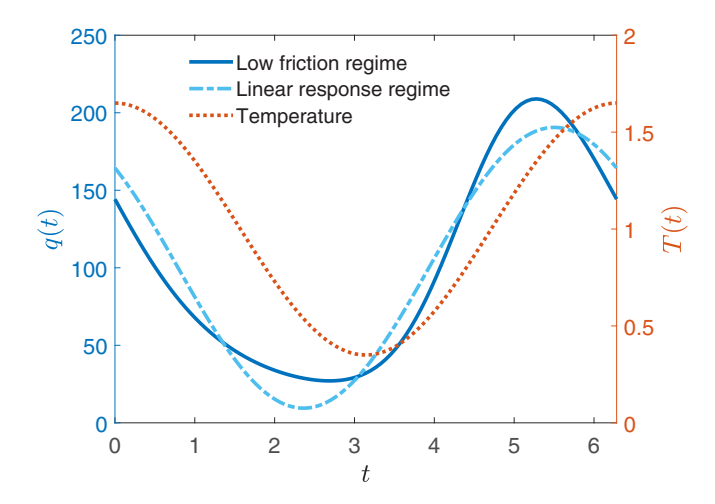


FIG. 2. Comparison between the optimal protocols q(t) in the low-friction and linear response regimes, for the sinusoidal temperature profile shown with a red-dotted curve.

terms become significant and the protocol is no longer optimal.

We finally highlight how the numerical value of power and efficiency, using the optimal protocol (13), deviates from the analytical expressions for maximum power (14) and efficiency at maximum power (21) with increasing values of the friction coefficient γ . This is shown in Fig. 4. Specifically, for small values of $\frac{\gamma}{\sqrt{mq}}$, the analytical and numerical results for power and efficiency coincide. For larger values of $\frac{\gamma}{\sqrt{mq}}$ the approximation error becomes significant due to the fact that the

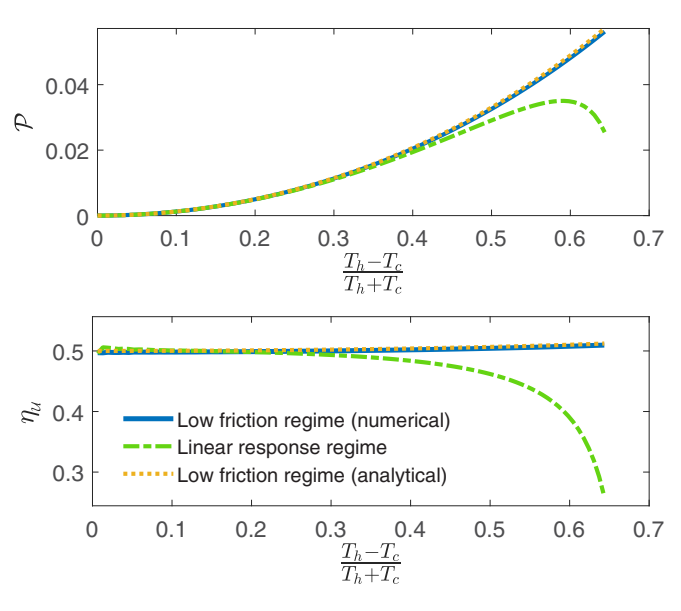


FIG. 3. Power and efficiency for (1) with a temperature profile (23) as functions of temperature ratios for two protocols: (i) the optimal protocol obtained under the low-friction assumption (13) (solid line), and (ii) the optimal protocol obtained in the linear response regime [31, Eqs. (29) and (30a)] (dashed line). For comparison, the analytical expressions for maximum power (14) and efficiency (21) in the low-friction regime are also drawn (dotted curve).

0.2

0

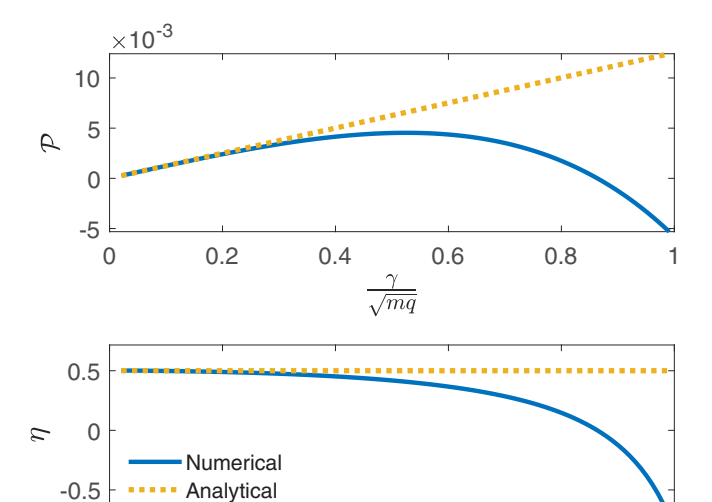


FIG. 4. Numerical values for power and efficiency as a function of the friction coefficient for the system governed by Eq. (4), driven by the optimal protocol (13) obtained in the low-friction regime (solid line). For comparison, we have included the analytical expressions for maximum power (14) and the efficiency at maximum power (21) obtained under the low-friction assumption (dotted line).

0.4

0.6

0.8

condition $\frac{\gamma}{\sqrt{mq}} \ll 1$, and hence, the approximate equipartition relation (5), no longer hold.

VI. CONCLUDING REMARKS

The present work quantifies maximum power, as well as the efficiency at any level of power, that can be achieved by a thermodynamic engine in the (underdamped) low-friction regime, modeled by a Langevin equation and in contact with a heat bath with periodic temperature profile.

It turns out that the maximum power and efficiency are expressed in terms of finite moments of the square root of the temperature profile. Moreover, when the temperature changes continuously, the optimal control protocol is expressed explicitly in terms of the temperature and certain finite moments, and is continuous in time as well.

Of particular interest is the efficiency at maximum power and, specifically, the relation between useful work and dissipation. Interestingly, when the third moment of the square root of the temperature profile is zero (for instance, due to a suitable time symmetry), at maximum power in the low-friction regime, the losses in dissipation equal the amount of work that can be extracted by the engine, yielding $\eta_{\iota \iota} = \frac{1}{2}$. It is of interest to explore possible connections of this result to the universal bound on the efficiency at maximum power being $\frac{1}{2}\eta_C$, where η_C is the Carnot efficiency [14,32].

ACKNOWLEDGMENTS

O.M.M., R.F., and A.T. contributed equally and A.T. oversaw the technical development. The research was partially supported by NSF under Grants No. 1807664, No. 1839441, No. 1901599, and No. 1942523 and AFOSR under Grant No. FA9550-20-1-0029.

- [1] S. Carnot, Reflexions on the Motive Power of Fire: A Critical Edition with the Surviving Scientific Manuscripts (Manchester University Press, Manchester, 1986).
- [2] C. J. Adkins, *Equilibrium Thermodynamics* (Cambridge University Press, Cambridge, UK, 1983).
- [3] K. Sekimoto, Stochastic Energetics (Springer, Berlin, 2010), Vol. 799.
- [4] U. Seifert, Stochastic thermodynamics, fluctuation theorems and molecular machines, Rep. Prog. Phys. **75**, 126001 (2012).
- [5] Y. Chen, T. Georgiou, and A. Tannenbaum, Stochastic control and non-equilibrium thermodynamics: Fundamental limits, IEEE Trans. Autom. Contr. 65, 2979 (2020).
- [6] C. Jarzynski, Equalities and inequalities: Irreversibility and the second law of thermodynamics at the nanoscale, Annu. Rev. Condens. Matter Phys. 2, 329 (2011).
- [7] C. Jarzynski, Nonequilibrium Equality for Free Energy Differences, Phys. Rev. Lett. **78**, 2690 (1997).
- [8] G. Gallavotti and E. G. D. Cohen, Dynamical Ensembles in Nonequilibrium Statistical Mechanics, Phys. Rev. Lett. 74, 2694 (1995).
- [9] D. J. Evans and D. J. Searles, Equilibrium microstates which generate second law violating steady states, Phys. Rev. E 50, 1645 (1994).

- [10] G. E. Crooks, Entropy production fluctuation theorem and the nonequilibrium work relation for free energy differences, Phys. Rev. E **60**, 2721 (1999).
- [11] T. Hatano and S. Sasa, Steady-State Thermodynamics of Langevin Systems, Phys. Rev. Lett. 86, 3463 (2001).
- [12] T. Schmiedl and U. Seifert, Efficiency at maximum power: An analytically solvable model for stochastic heat engines, Europhys. Lett. **81**, 20003 (2007).
- [13] R. Fu, A. Taghvaei, Y. Chen, and T. T. Georgiou, Maximal power output of a stochastic thermodynamic engine, Automatica **123**, 109366 (2021).
- [14] C. Van den Broeck, Thermodynamic Efficiency at Maximum Power, Phys. Rev. Lett. 95, 190602 (2005).
- [15] A. Dechant, N. Kiesel, and E. Lutz, Underdamped stochastic heat engine at maximum efficiency, Europhys. Lett. 119, 50003 (2017).
- [16] N. Zöller, Optimization of Stochastic Heat Engines in the Underdamped Limit (Springer, Berlin, 2017).
- [17] V. Blickle and C. Bechinger, Realization of a micrometre-sized stochastic heat engine, Nat. Phys. 8, 143 (2012).
- [18] O. Abah, J. Roßnagel, G. Jacob, S. Deffner, F. Schmidt-Kaler, K. Singer, and E. Lutz, Single-Ion Heat Engine at Maximum Power, Phys. Rev. Lett. 109, 203006 (2012).

- [19] I. A. Martínez, E. Roldán, L. Dinis, D. Petrov, and R. A. Rica, Adiabatic Processes Realized with a Trapped Brownian Particle, Phys. Rev. Lett. 114, 120601 (2015).
- [20] V. Cilek, Earth System: History and Natural Variability-Volume III, Vol. 3 (EOLSS, Abu Dhabi, UAE, 2009).
- [21] T. Yanagida, M. Ueda, T. Murata, S. Esaki, and Y. Ishii, Brownian motion, fluctuation and life, Biosystems **88**, 228 (2007).
- [22] E. Schrödinger, What is life?, *The Physical Aspect of the Living Cell* (Cambridge University Press, Cambridge, 1944).
- [23] S. Ornes, Core concept: How nonequilibrium thermodynamics speaks to the mystery of life, Proc. Natl. Acad. Sci. USA 114, 423 (2017).
- [24] M. Bauer, K. Brandner, and U. Seifert, Optimal performance of periodically driven, stochastic heat engines under limited control, Phys. Rev. E **93**, 042112 (2016).
- [25] K. Brandner, K. Saito, and U. Seifert, Thermodynamics of Micro- and Nano-Systems Driven by Periodic Temperature Variations, Phys. Rev. X 5, 031019 (2015).

- [26] K. Brandner and K. Saito, Thermodynamic Geometry of Microscopic Heat Engines, Phys. Rev. Lett. 124, 040602 (2020).
- [27] A. Dechant, N. Kiesel, and E. Lutz, All-Optical Nanomechanical Heat Engine, Phys. Rev. Lett. 114, 183602 (2015).
- [28] A. Gomez-Marin, T. Schmiedl, and U. Seifert, Optimal protocols for minimal work processes in underdamped stochastic thermodynamics, J. Chem. Phys. **129**, 024114 (2008).
- [29] I. I. Novikov, The efficiency of atomic power stations (a review), J. Nucl. Energy 7, 125 (1958).
- [30] F. L. Curzon and B. Ahlborn, Efficiency of a Carnot engine at maximum power output, Am. J. Phys. 43, 22 (1975).
- [31] R. Fu, O. M. Miangolarra, A. Taghvaei, Y. Chen, and T. T. Georgiou, Harvesting energy from a periodic heat bath, in *Proceedings of the 2020 59th IEEE Conference on Decision and Control (CDC'20)* (IEEE, Los Alamitos, CA, 2020), pp. 3034–3039.
- [32] M. Esposito, K. Lindenberg, and C. Van den Broeck, Universality of Efficiency at Maximum Power, Phys. Rev. Lett. 102, 130602 (2009).